Phosphoinositide Metabolism and the Morphology of Human Erythrocytes

JAMES E. FERRELL, JR. and WRAY H. HUESTIS
Department of Chemistry, Stanford University, Stanford, California 94305

ABSTRACT ATP-depleted human erythrocytes lose their smooth discoid shape and adopt a spiny, crenated form. This shape change coincides with the conversion of phosphatidylinositol-4,5-bisphosphate to phosphatidylinositol and phosphatidic acid to diacylglycerol. Both crenation and lipid dephosphorylation are accelerated by iodoacetamide, and both are reversed by nutrient supplementation. The observed changes in lipid populations should shrink the membrane inner monolayer by 0.6%, consistent with estimates of bilayer imbalance in crenated cells. These observations suggest that metabolic crenation arises from a loss of inner monolayer area secondary to the degradation of phosphatidylinositol-4,5-bisphosphate and phosphatidic acid. A related process, crenation after Ca^{2+} loading, appears to arise from a loss of inositides by a different pathway.

The shape of human erythrocytes is under metabolic control; after cells exhaust their ATP they become spiculate spheres. This shape change (called crenation or echinocytosis) eventually becomes irreversible, but for many hours crenated cells can revert to normal discoid shape if ATP is restored by appropriate nutrients (1).

Certain amphipathic molecules induce shape changes similar to metabolic crenation in ATP-replete cells, whereas other amphipaths produce what appears to be the reverse process, stomatocytosis. To explain the morphological effects of amphipaths, Sheetz and Singer (2) proposed the bilayer couple hypothesis, which attributes cell shape to the relative areas of the plasma membrane monolayers. According to this model, cationic amphipaths capable of rapid trans-bilayer flip-flop (e.g., chlorpromazine) would be expected to bind preferentially to the acidic phospholipids of the inner leaflet, expanding its area and causing the cell to cup. Anionic amphipaths (e.g., barbiturates) and molecules incapable of fast flip-flop (e.g., methochlorpromazine) should accumulate in the outer leaflet, expanding it and thereby producing the spiny shape of echinocytes. Although serious objections to this model have been raised (3) and countered (4, 5), it is indisputable that the bilayer couple hypothesis successfully predicts the morphological effects of a wide variety of drugs. However, it is not apparent how metabolic depletion might induce bilayer imbalance.

Other workers have suggested that erythrocyte shape might be controlled by the membrane protein cytoskeleton acting as a scaffolding upon which the rest of the membrane is built. Circumstantial support for this idea arose from studies of Triton shells, the proteinaceous remains of detergent-treated ghosts. Early reports (6–8) indicated that these cytoskeletal shells retain the shape of the cell from which they are derived (discocytic, elliptocytic, irreversibly sickled), suggesting that they possess a long-term morphological memory.

Subsequent work by Sheetz, Birchmeier, and Singer (9, 10) provided further support for the idea that the cytoskeleton controls red cell shape, and suggested how ATP depletion leads to crenation. They proposed that metabolic control of the cytoskeleton is exerted through the phosphorylation and dephosphorylation of the β-subunit of the protein spectrin. This assertion was supported by Pinder et al. (11) who found that the viscosity of crude mixtures of spectrin and other cytoskeletal components varies with the degree of spectrin phosphorylation. ATP depletion would lead to spectrin dephosphorylation, which was thought to rearrange the cytoskeleton and contract the inner monolayer (10). The resulting bilayer imbalance would force the cell to crenate.

This hypothesis was largely confuted by three observations. First, α-adrenergic stimulation increases spectrin phosphorylation without detectable morphological consequences (12). Second, much of the spectrin kinase activity of ghosts can be extracted or inhibited without altering their capacity to become discoid (13, 14). Finally, if spectrin dephosphorylation were to cause metabolic crenation, it should either precede the shape change or occur concurrently. Anderson and Tyler (15) showed that in intact cells, spectrin dephosphorylation lags behind metabolic crenation. These observations all show

THE JOURNAL OF CELL BIOLOGY · VOLUME 98 JUNE 1984 1992–1998

that there is no simple relationship between spectrin phosphorylation and cell shape. Indeed, it has yet to be demonstrated that spectrin phosphorylation has any functional consequences (15, 16).

Recently Lange and co-workers (17, 18) have found that Triton shells do not always echo the shape of the parent cell. These workers concluded that the cytoskeleton probably does not control cell shape. Rather, previously noted similarities between cells and Triton shells could reflect the tendency of the cytoskeletal reticulum to conform (with short-term elasticity and long-term plasticity) to the shape dictated by the lipid bilayer.

In 1975, Allan and Michell (19) found elevated levels of diacylglycerol in echinocytes formed by either metabolic depletion or calcium loading. They proposed that this lipid triggers crenation, and that its fusogenic activity induces the membrane budding (microvesiculation) observed subsequent to crenation. Later, they and their co-workers showed that calcium loading activates a phospholipase C, which degrades phosphatidylinositol-4-phosphate and phosphatidylinositol-4,5-bisphosphate. In ATP-replete cells, the resulting diacylglycerol is quickly phosphorylated to yield phosphatidic acid, while crenation proceeds (20). This observation negated the hypothesis that diacylglycerol accumulation per se causes crenation, but left open the possibility that related processes might be involved in morphology changes.

In this report, we examine inositide metabolism during both metabolic crenation and its reversal. Our findings support the conclusion that metabolic crenation is caused by lipid bilayer imbalance secondary to the loss of phosphatidylinositol-4,5-bisphosphate and phosphatidic acid from the inner monolayer of the cell membrane.

MATERIALS AND METHODS

Human erythrocytes were obtained by venipuncture, pelleted by centrifugation, and washed three times with 4 vol of 150 mM NaCl and once with 138 mM NaCl, 5 mM KCl, 6.1 mM Na_2HPO_4, 1.4 mM NaH_2PO_4, 1 mM $MgSO_4$, 5 mM glucose, pH 7.4 ($NaCl/P_i$). Cells were used within 6 h of being drawn. All of the incubations described below were carried out at 37°C, hematocrit 20, in capped plastic tubes.

Prelabeling Cells with ^{32}P

Erythrocytes were labeled with ^{32}P by incubation for 18–30 h with $NaCl/P_i$ supplemented with 10 mM inosine, 1 mM adenosine, and an additional 5 mM glucose (supplemented $NaCl/P_i$). The suspension medium contained antibiotics to retard bacterial growth (penicillin G, 100 μg/ml, plus either streptomycin, 100 μg/ml, or tobramycin, 40 μg/ml) and ~25 μCi/ml $[^{32}P]H_3PO_4$ (ICN Nutritional Biochemicals, Cleveland, OH, carrier-free). In one experiment, supplemented $NaCl/P_i$ was replaced with $NaCl/P_i$, to which 10 mM glucose was added every 7–8 h. This protocol maintained ATP levels less well than the first procedure, but the results of the experiment were otherwise similar to the results of a duplicate experiment using supplemented $NaCl/P_i$. Incubations of this length allowed equilibration of ATP, phosphatidylinositol-4-phosphate, and phosphatidylinositol-4,5-bisphosphate (but not phosphatidic acid) with the radiolabeled phosphate.

Metabolic Depletion and Repletion

Metabolic depletion was initiated by one of two procedures. (*a*) Slow ATP depletion: ^{32}P-labeled cells were pelleted, washed once in 4 vol of 150 mM NaCl, and resuspended in 140 mM NaCl, 10 mM HEPES, pH 7.4, plus penicillin G (100 μg/ml) and tobramycin (40 μg/ml). This treatment induces ATP depletion and crenation with half-times of ~12 and 34 h, respectively. (*b*) Rapid ATP depletion: ^{32}P-labeled cells were pelleted, washed three times in 4 vol of 150 mM NaCl, and resuspended in 140 mM NaCl, 10 mM HEPES, 10 mM inosine, 6 mM iodoacetamide, pH 7.4. In this medium, cells deplete their ATP within 1 h, and crenation follows rapidly (21).

The reversal of metabolic crenation was examined in echinocytes produced by procedure *a*. The echinocytes were pelleted, washed once in $NaCl/P_i$, and resuspended in supplemented $NaCl/[^{32}P]P_i$, a portion of which had been used in the prelabeling phase of the experiment.

Assay Procedures

MORPHOLOGY: Erythrocytes were diluted to hematocrit 5 and fixed in 150 mM NaCl containing 0.5% glutaraldehyde (Sigma Chemical Co., St. Louis, MO) for 5 min, which precludes the "glass effect" (22). Cell samples were then examined by bright field microscopy with oblique illumination, a procedure that makes the cell image appear three dimensional (23). Some cell samples were placed on Nuclepore filters (Pleasanton, CA), freeze-dried, sputter-coated, and examined by scanning electron microscopy. Echinocytes were assigned a morphology score of 1–5 based on Bessis's nomenclature for echinocytes and spheroechinocytes (22). Discocytes were assigned a score of 0, and stage I stomatocytes, observed in a few fields, were assigned a score of −1. The average score for a field of 100 cells was called its morphological index (MI).[1]

ATP: Frozen aliquots of cell suspension (50 μl) were diluted in 2.45 ml of 150 mM NaCl, boiled for 15 min, and centrifuged to clarity. The supernatant (diluted 1:10 or undiluted) was assayed for ATP by the luciferin-luciferase (Calbiochem-Behring Corp., San Diego, CA) method (24).

LIPIDS: Frozen aliquots of cell suspension (100 μl) were lysed in 1 ml cold 10 mM Tris/2 mM EDTA, pH 7.5, to prevent hydrolysis of radiolabeled lipids (25, 26). Samples were centrifuged for 5 min at 8,800 *g*, and the pellets were washed once in Tris/EDTA. The entire ghost pellet was extracted with 100:50:1 (vol/vol) methanol/chloroform/concentrated HCl (1.8 ml) followed by water (0.6 ml) and chloroform (0.6 ml). The organic phase was reserved and the aqueous phase extracted again with 1.2 ml chloroform. The organic phases were combined, dried under a stream of nitrogen, and dissolved in two 10-μl portions of chloroform. Lipids were separated by thin-layer chromatography (TLC) on 2.5 × 10-cm plates in two solvent systems. (*a*) Silica Gel HL (Analtech, Inc., Newark, DE; not activated) developed in 48:40:10:5 (vol/vol) methanol/chloroform/water/concentrated NH_3 separated the inositides from the origin and resolved the three radioactive lipids (Fig. 1). Typical R_f values were phosphatidylinositol-4,5-bisphosphate, 0.38; phosphatidylinositol-4-phosphate, 0.46; lysophosphatidylcholine, 0.56; phosphatidic acid and heme, 0.60; sphingomyelin, phosphatidylserine, phosphatidylinositol, and lysophosphatidylethanolamine, 0.60–0.66; phosphatidylcholine, 0.72; phosphatidylethanolamine, 0.79; and cholesterol, 0.98. (*b*) Diacylglycerol was separated from other neutral lipids on Silica Gel G (Analtech; not activated) developed in 25:20:1:0.1 (vol/vol) benzene/diethyl ether/ethanol/acetic acid. Phospholipids remained at the origin; typical R_f values were unsaturated fatty acids, 0.48; cholesterol, 0.53; saturated fatty acids, 0.64; and diacylglycerol, 0.70. Lipid spots were detected with iodine vapor. Radiolabeled phospholipids were detected by autoradiography using Kodak X-OMAT AR film (Eastman Kodak Co., Rochester, NY) with a Dupont Cronex intensifying screen (DuPont Instruments, Wilmington, DE) (Fig. 1 *a*), and quantified by liquid scintillation counting of scraped spots.

Lipid phosphorus in phosphatidylinositol-4-phosphate and phosphatidylinositol-4,5-bisphosphate and total lipid phosphate were determined by a small scale adaptation of the spectrophotometric method of Bartlett, corrected for silica background (27). No one-dimensional TLC system tested separated phosphatidylinositol and phosphatidic acid from the major phospholipids well enough to allow accurate phosphate determinations. This separation was accomplished by two-dimensional TLC on 10 × 10 cm Silica Gel HL (Analtech) plates. The solvent systems used were 65:25:5 (vol/vol) chloroform/methanol/concentrated NH_3 followed by 65:50:5 (vol/vol) chloroform/methanol/acetic acid to separate phosphatidylinositol (Fig. 1 *b*), and 60:30:6 (vol/vol) chloroform:methanol:concentrated NH_3 followed by 60:10:6 (vol/vol) chloroform/methanol/acetic acid to separate phosphatidic acid (Fig. 1 *c*). Both two-dimensional systems also afforded good separation of the major phospholipids.

RESULTS

Lipids were extracted from fresh human erythrocytes and the molar percentages of each phospholipid class were measured by phosphate assay. Table I summarizes the results of 6 one-dimensional and 24 two-dimensional TLC separations. The proportions of the major phospholipids agree well with previously reported values (28, 29) except for phosphatidylinositol-4,5-bisphosphate; whereas Allan and Michell found 0.4

[1] *Abbreviations used in this paper*: MI, morphological index; TLC, thin layer chromatography.

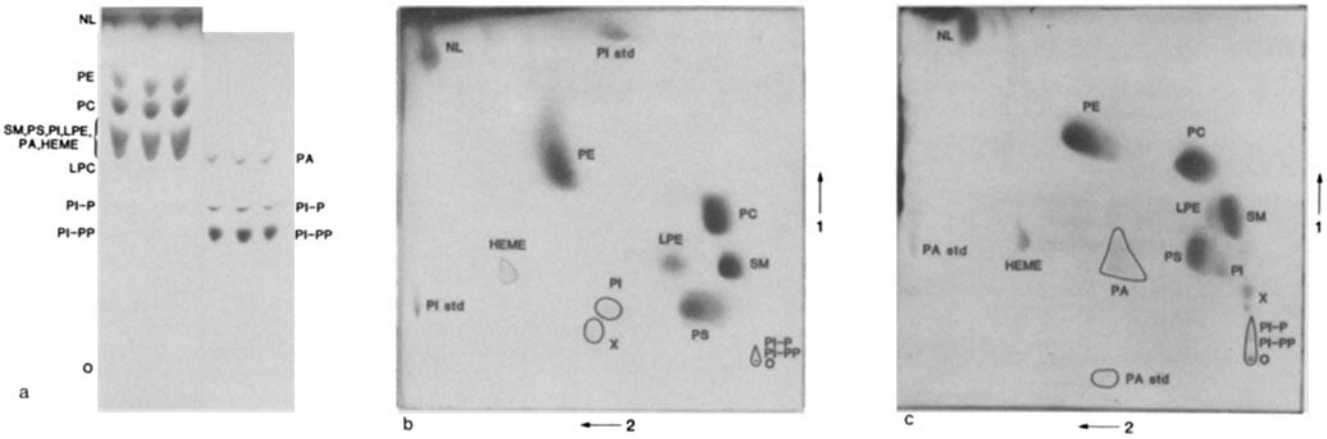

FIGURE 1 TLC separations of lipid extracts from human erythrocytes. (*a*) One-dimensional development in 48:40:10:5 (vol/vol) methanol/chloroform/water/concentrated NH_3. Lipid spots were detected by iodine vapor (*left*); ^{32}P-labeled lipids were detected by autoradiography (*right*). *O*, origin; *PI-PP*, phosphatidylinositol-4,5-bisphosphate; *PI-P*, phosphatidylinositol-4-phosphate; *LPC*, lysophosphatidylcholine; *SM*, sphingomyelin; *PS*, phosphatidylserine; *PI*, phosphatidylinositol; *LPE* lysophosphatidylethanolamine; *PA*, phosphatidic acid; *PC*, phosphatidylcholine; *PE*, phosphatidylethanolamine; *NL*, neutral lipids. (*b*) Two-dimensional development in 65:25:5 (vol/vol) chloroform/methanol/concentrated NH_3 followed by 65:50:5 (vol/vol) chloroform/methanol/acetic acid, detected by iodine vapor. *X* is an unidentified lipid spot containing <0.1% of total lipid phosphate. (*c*) Two-dimensional development in 60:30:6 (vol/vol) chloroform/methanol/concentrated NH_3 followed by 60:10:6 (vol/vol) chloroform/methanol/acetic acid, detected by iodine vapor. *X* represents unidentified lysolipids.

± 0.07%, we find 1.4 ± 0.3%. It is possible that their lower value reflects partial hydrolysis during their more extensive lysis and washing procedures (28).

As has been reported (28), red cells incubated with [^{32}P]-PO_4 and nutrients incorporated detectable radiolabel into phosphatidylinositol-4-phosphate, phosphatidylinositol-4,5-bisphosphate, and phosphatidic acid, but not into other phospholipids (Fig. 1 *a*). The radiolabel equilibrated with phosphatidylinositol-4-phosphate and phosphatidylinositol-4,5-bisphosphate in 15–25 h, approximately the time scale on which it equilibrates with ATP (15, 30). In contrast, phosphatidic acid equilibrated more slowly, with [^{32}P]phosphatidic acid increasing steadily through 50 h of incubation even as ATP levels fell to a few percent of normal. This indicates that phosphatidic acid turnover is slow and that the diacylglycerol kinase remains active even at very low ATP levels.

The ratio of [^{32}P]phosphatidylinositol-4,5-bisphosphate to [^{32}P]phosphatidylinositol-4-phosphate fell somewhat during the prelabeling, indicating that the 5-phosphate equilibrates more rapidly than the 4-phosphate, in agreement with a previous report (31). The amounts of radiolabel incorporated into phosphatidylinositol-4,5-bisphosphate and phosphatidylinositol-4-phosphate at equilibrium indicate a molar ratio of 1.8 ± 0.3 (assuming two exchangeable phosphates per phosphatidylinositol-4,5-bisphosphate molecule and one per phosphatidylinositol-4-phosphate), in good agreement with the ratio obtained by phosphate assay (1.5 ± 0.4).

TABLE I

Phospholipid Composition of Human Erythrocytes

Phospholipid class	Molar percentage	*n*
	%	
Phosphatidylinositol-4,5-bisphosphate	1.4 ± 0.3	6
Phosphatidylinositol-4-phosphate	0.8 ± 0.3	6
Phosphatidylinositol	1.2 ± 0.1	4
Phosphatidic acid	2.2 ± 0.2	6
Sphingomyelin	24.5 ± 2.0	24
Phosphatidylcholine	25.4 ± 1.1	24
Phosphatidylserine	15.8 ± 1.7	24
Phosphatidylethanolamine	27.0 ± 1.7	24
Lysophosphatidylcholine	1.0 ± 0.3	24
Lysophosphatidylethanolamine	1.3 ± 1.0	24
Total	100.6	

Phospholipids were extracted from fresh cells or cells incubated for 15–30 h with supplemented NaCl/[^{32}P]P_i. Lipids were separated by one-dimensional (phosphatidylinositol-4-phosphate and phosphatidylinositol-4,5-bisphosphate) or two-dimensional TLC, and quantified by phosphate assay. Values shown are means ± SD.

Slow Metabolic Crenation

Erythrocytes labeled with ^{32}P were allowed to deplete their ATP slowly. After a lag of ~15 h, the cells began to crenate, leveling off at a morphological index of +3 after 45 h of incubation (Figs. 2 and 3). This shape change coincided with a 70% decrease in phosphatidylinositol-4,5-bisphosphate (Fig. 3 *b*). Phosphatidylinositol-4-phosphate levels did not change significantly.

In separate experiments, unlabeled erythrocytes were allowed to deplete their ATP and their levels of phosphatidylinositol and phosphatidic acid were measured. After a lag, crenation proceeded at the same rate and to the same extent as for radiolabeled cells. The level of phosphatidylinositol nearly doubled, with its increase mirroring the previously noted drop in phosphatidylinositol-4,5-bisphosphate (Fig. 3 *b*). Phosphatidic acid levels dropped by ~20%, accompanied by a qualitative increase in diacylglycerol. No changes in the levels of sphingomyelin, phosphatidylcholine, phosphatidylserine, phosphatidylethanolamine, lysophosphatidylcholine, or lysophosphatidylethanolamine were detected.

Recovery of the Discoid Shape

At two points during slow crenation, cells were pelleted, washed, and resuspended in supplemented NaCl/[^{32}P]P_i. After

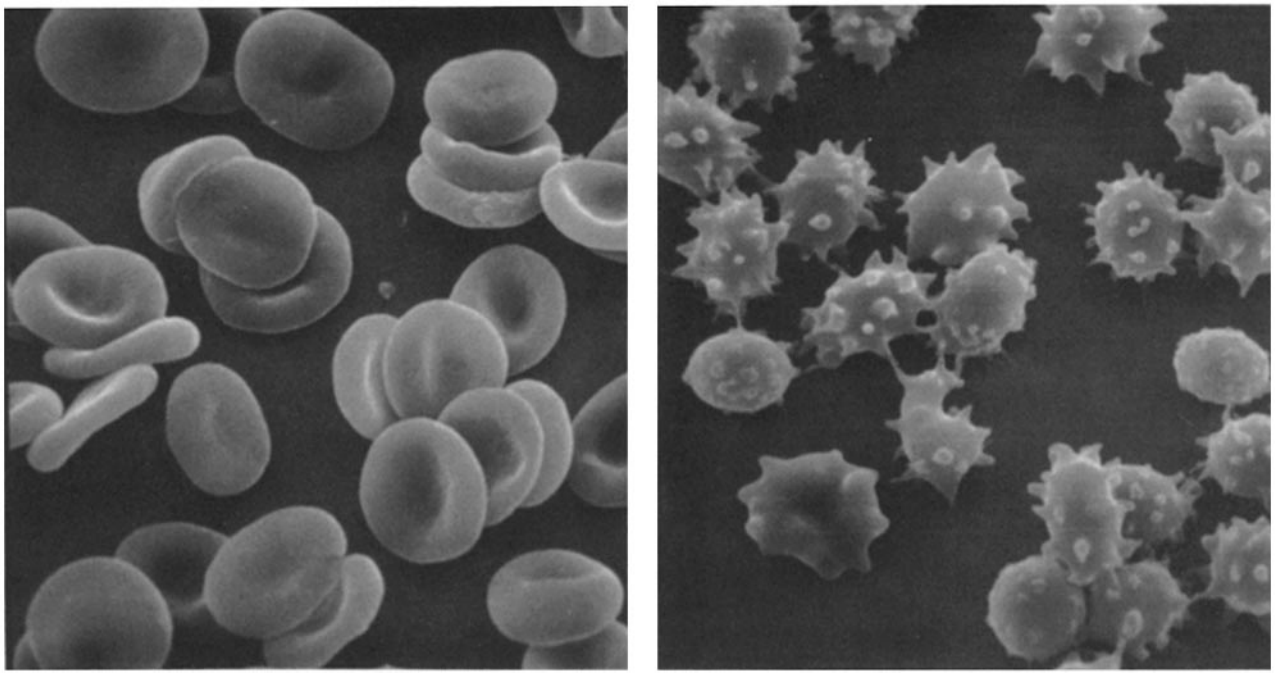

FIGURE 2 (*Top*) Scanning electron micrographs of fresh discocytes (*left*) and echinocytes formed by 30 h of metabolic depletion (*right*). × 3000. (*Bottom*) Morphology grading scale, based on the nomenclature of Bessis (22).

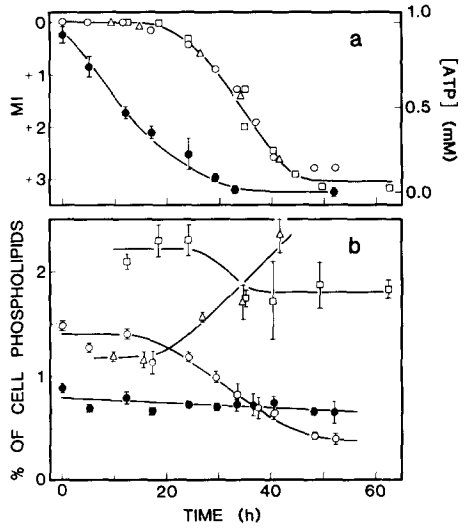

FIGURE 3 Slow metabolic crenation. (a) After cells were washed free of sugar, ATP levels fell (●) and the cells crenated (○, □, △). (*b*) As the cells changed shape, phosphatidylinositol-4,5-bisphosphate levels decreased (○) and phosphatidylinositol levels increased (△). Phosphatidic acid levels fell by a smaller amount (□) and phosphatidylinositol-4-phosphate fell only slightly (●). These data were taken from three experiments: one to assay ATP (●), shape (○), and radiolabeled phosphatidylinositol-4-phosphate (●) and phosphatidylinositol-4,5-bisphosphate (○); one to assay shape and phosphatidylinositol (△); and one to assay shape and phosphatidic acid (□). The zero time-point was taken to be the beginning of ATP depletion in the first experiment. In the other two experiments, the shape changes occurred at similar rates and to similar extents, but with somewhat different lag times. To facilitate comparison, the time scales for the latter experiments were shifted so that the shape changes from all three corresponded. In Figs. 3–5, the data shown for the radiolabeled phospholipids were calculated by converting ^{32}P counts to moles of lipid (determined by phosphate assay), and then to percentage of total cell phospholipid. Error bars in this and all subsequent figures represent 1 SE.

33 h of depletion, this nutrient supplementation allowed the cells to regenerate ~20% of their ATP (Fig. 4*a*). Subsequently, the echinocytes (MI = +1.7) converted to discocytes and a few stage I stomatocytes (Fig. 4*a*). This shape recovery was accompanied by an increase in phosphatidylinositol-4,5-bisphosphate levels from ~85% to 125% of normal, and a decrease in phosphatidylinositol-4-phosphate (Fig. 4*b*). There was no detectable change in phosphatidic acid levels.

A second nutrient supplementation was begun after 46 h of metabolic depletion. [ATP] rose more slowly and leveled off at 6% of normal (Fig. 4*c*), which was sufficient to allow the cells to revert from MI = +2.9 to MI = +0.4. The shape recovery began ~30 min after the nutrients were added and leveled off after 3–4 h. After a similar time lag, phosphatidylinositol-4,5-bisphosphate levels rose to ~80% of normal at 2 h (Fig. 4*d*). This increase was accompanied by an increase in phosphatidic acid to normal levels, and a decrease in phosphatidylinositol-4-phosphate levels.

Rapid Metabolic Crenation

Radiolabeled cells treated with inosine and iodoacetamide depleted their ATP in ~1 h. As shown in Fig. 5, a decrease in phosphatidylinositol-4,5-bisphosphate once again coincided with crenation. Both the shape change (ΔMI = +2) and the decrease in phosphatidylinositol-4,5-bisphosphate (40%) were

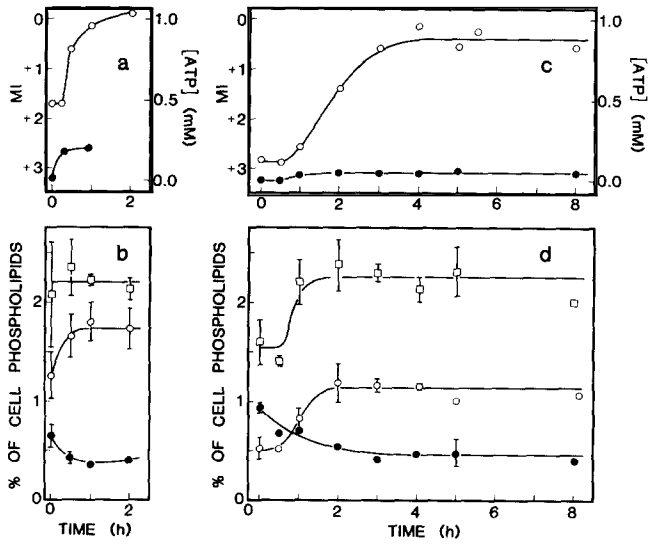

FIGURE 4 Shape recovery in crenated cells. (*a*) Erythrocytes were metabolically depleted for 33 h, then resuspended in supplemented NaCl/P_i. ATP levels rose (●) and the cells recovered their normal shape (○). (*b*) Lipid levels during the shape recovery showing an increase in phosphatidylinositol-4,5-bisphosphate (○), a decrease in phosphatidylinositol-4-phosphate (●), and no significant change in phosphatidic acid (□). (*c*) Erythrocytes were metabolically depleted for 46 h, then resuspended in supplemented NaCl/P_i. ATP level rose slightly (●) and the cells partially recovered their normal shape (○). During this shape recovery (*d*) phosphatidylinositol-4,5-bisphosphate (○) and phosphatidic acid (□) levels rose, while phosphatidylinositol-4-phosphate levels fell (●).

smaller than those observed in slow metabolic crenation, and both leveled off at ~8 h. Phosphatidic acid levels fell slightly, and phosphatidylinositol-4-phosphate levels appeared to remain constant.

DISCUSSION

Metabolism of Lipids during Metabolic Crenation and Shape Recovery

Fig. 6 summarizes the known metabolic pathways of phosphatidic acid and the inositides in human erythrocytes. At least two pairs of kinases and phosphatases interconvert phosphatidylinositol, phosphatidylinositol-4-phosphate, and phosphatidylinositol-4,5-bisphosphate (26, 31), and another pair interconverts diacylglycerol and phosphatidic acid (32, 33). In addition, both phosphatidylinositol-4-phosphate and phosphatidylinositol-4,5-bis-phosphate can be hydrolyzed to diacylglycerol by a Ca^{2+}-dependent phospholipase C (28).

The absolute amount of phosphatidylinositol-4,5-bisphosphate degraded during slow metabolic depletion corresponds closely to the amount of phosphatidylinositol formed (Fig. 3), suggesting that phosphatidylinositol-4,5-bisphosphate is degraded by phosphomonesterases. This conclusion is supported by the previous demonstration that metabolic depletion engenders smaller increases in intracellular Ca^{2+} (<1 μM) than the 100 μM required to activate the phospholipase C (34). Phosphatidylinositol-4-phosphate levels do not change, indicating that either the phosphatidylinositol-4,5-bisphosphate phosphatase and phosphatidylinositol-4-phosphate phosphatase operate at similar rates, or that phosphatidylinositol-4,5-bisphosphate is degraded to phosphatidylinositol by a route that does not involve phosphatidylinositol-4-phosphate (for example, conversion of phosphatidylinositol-4,5-bisphosphate to phosphatidylinositol-5-phosphate, followed by its rapid degradation to phosphatidylinositol). Slow crenation was also accompanied by a small decrease in phosphatidic acid, implying conversion to diacylglycerol via phosphatidic acid phosphatase. Rapid ATP depletion effected more rapid and less extensive lipid degradation (Fig. 5), as well as a more rapid and less extensive shape change.

The lipid metabolism accompanying crenation appeared to be more or less reversed during shape recovery. Phosphatidic acid was restored to normal levels, and phosphatidylinositol-4,5-bisphosphate was restored to 125% (Fig. 4*b*) and 80% (Fig. 4*d*) of normal. The increase in phosphatidylinositol-4,5-bisphosphate levels was accompanied by a decrease in phosphatidylinositol-4-phosphate that was somewhat smaller in

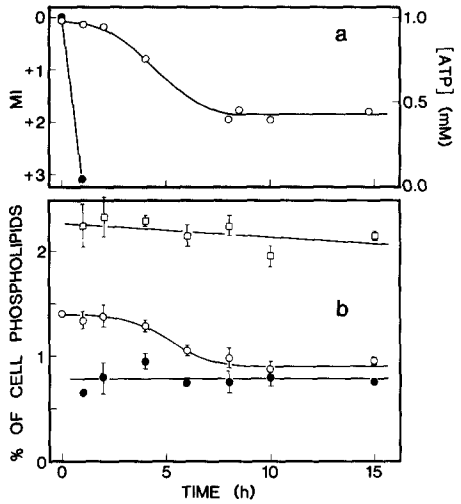

FIGURE 5 Iodoacetamide-induced metabolic crenation. (*a*) ATP levels fell rapidly (●), and the cells crenated a few hours later (○). (*b*) Lipid levels changed more rapidly and less extensively than during slow metabolic crenation. Phosphatidylinositol-4,5-bisphosphate levels fell (○); phosphatidic acid fell slightly (□); and phosphatidylinositol-4-phosphate remained constant (●).

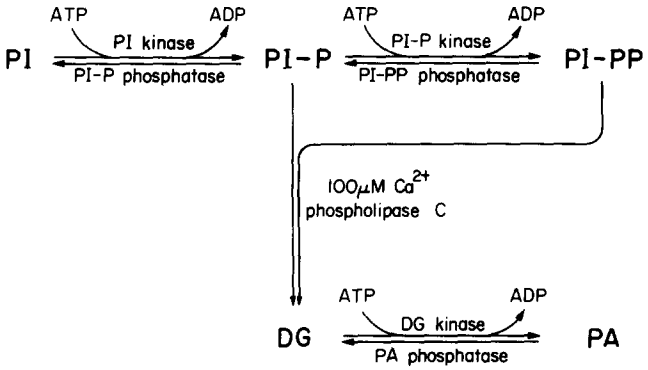

FIGURE 6 Pathways of inositide metabolism. Three pairs of kinases and phosphomonesterases are thought to interconvert the inositides (*PI, PI-P, PI-PP*), diacylglycerol (*DG*), and phosphatidic acid (*PA*). High levels of intracellular calcium activate a Ca^{2+}-dependent phospholipase C, which degrades phosphatidylinositol-4-phosphate and phosphatidylinositol-4,5-bisphosphate to diacylglycerol. During metabolic crenation lipid metabolism is shifted in favor of diacylglycerol and phosphatidylinositol. The phospholipase C does not appear to be activated. During shape recovery in echinocytes, phosphatidylinositol-4,5-bisphosphate and phosphatidic acid are resynthesized.

absolute terms, implying that some phosphorylation of phosphatidylinositol was also taking place.

During both slow and rapid metabolic depletion, lipid changes paralleled the cell shape changes. During repletion, the shape recovery lagged perhaps 30–60 min behind lipid phosphorylation, still a close temporal association. The correlation between crenation and inositide breakdown also holds for the extremely rapid crenation induced by calcium loading. Allan and Thomas (20) reported that erythrocytes incubated with 1 mM Ca^{2+} and 5 μM A23187 (at hematocrit 20 in 130 mM NaCl/20 mM 3-[*N*-morpholino]propane sulfonic acid, pH 7.1) lose 70% of their phosphatidylinositol-4-phosphate and phosphatidylinositol-4,5-bisphosphate with a half-time of 4 min. Under the same conditions, we observe that cells crenate with a similar half-time of 2 min.

These results demonstrate that phosphatidylinositol-4,5-bisphosphate (and perhaps phosphatidic acid) is degraded or synthesized concomitantly with five shape changes whose characteristic times vary over three orders of magnitude (Table II). It is improbable that these associations are fortuitous, suggesting a causative link between lipid dephosphorylation and crenation. Further, inositide breakdown appears to mediate both metabolic crenation and Ca^{2+} crenation, but by different pathways: phosphomonesterases in metabolic crenation and the Ca^{2+}-dependent phospholipase C in Ca^{2+} crenation.

Lipid Changes and Bilayer Imbalance

Phosphatidylinositol-4,5-bisphosphate is thought to reside exclusively in the inner monolayer of the red cell membrane. It is highly polar and should flip-flop only very slowly. During crenation, phosphatidylinositol-4,5-bisphosphate is converted to phosphatidylinositol, which has a smaller, less highly charged headgroup. Thus, breakdown of phosphatidylinositol-4,5-bisphosphate would be expected to shrink the inner monolayer, even assuming that phosphatidylinositol, like phosphatidylinositol-4,5-bisphosphate, does not flip-flop. We can estimate roughly the amount of inner monolayer contraction this change should produce.

The concentration of phospholipids in packed red cells is 3.6 mM (35). Assuming a red cell volume of 88 fl, this concentration corresponds to 1.9×10^8 phospholipid molecules per cell, of which 1.4% or 2.7×10^6 molecules per cell are phosphatidylinositol-4,5-bisphosphate. About 70% of these, 1.9×10^6 molecules per cell, are degraded to phosphatidylinositol during slow metabolic crenation.

The membrane surface area normally occupied by a molecule of phosphatidylinositol-4,5-bisphosphate has not been measured. Based on x-ray diffraction studies of phosphatidylcholine (36) and molecular models, we estimate that phosphatidylinositol-4,5-bisphosphate occupies ~0.6–0.9 nm^2 per molecule, with phosphatidylinositol ~0.25 nm^2 smaller. Thus, the conversion of 1.9×10^6 molecules of phosphatidylinositol-4,5-bisphosphate to phosphatidylinositol would entail the loss of ~0.48 μm^2 of inner monolayer surface area. Taking the surface area of an erythrocyte to be 140 μm^2, this is a 0.33% contraction. A larger contraction would result if some of the newly formed phosphatidylinositol flip-flopped to the outer monolayer.

TABLE II

Correspondence between Lipid and Shape Changes

Process	$t_{1/2}$ Lipid change	$t_{1/2}$ Shape change
Slow metabolic crenation	31 h	33 h
Rapid metabolic crenation	5 h	4–5 h
Recovery from MI = +1.7 to −0.1	15 min	25 min
Recovery from MI = +2.9 to +0.4	60 min	105 min
Ca^{2+} crenation	4 min*	2 min

* Taken from reference 20.

The small amounts of phosphatidic acid converted to diacylglycerol during metabolic crenation should also contribute to the contraction of the inner monolayer. Assuming that the diacylglycerol flip-flops rapidly (37) and distributes evenly between the monolayers, a 20% decrease in phosphatidic acid levels should produce a 0.32% contraction of the inner monolayer. In total, the conversion of phosphatidylinositol-4,5-bisphosphate to phosphatidylinositol and phosphatidic acid to diacylglycerol during slow metabolic depletion would be expected to shrink the inner monolayer by 0.65%.

This estimate, while approximate, agrees well with both theoretical and experimental estimates of the bilayer imbalance needed to produce stage 3 echinocytes. An early report of inner and outer monolayer surface areas calculated from geometrical models predicted that a shift in the bilayer balance of 0.4% should convert discocytes to stage 3 echinocytes (38). Further calculations (Ferrell, J. E., K. J. Lee, and W. H. Huestis, manuscript in preparation) and a recent experimental study (39) suggest that ~1.2% expansion of the outer monolayer is necessary to produce this degree of shape change.

It is possible that phosphatidylinositol-4,5-bisphosphate plays some role in regulating red cell shape beyond its mere occupancy of inner monolayer area. Inositides, and phosphatidylinositol-4,5-bisphosphate in particular, bind avidly to certain proteins. Disappearance of phosphatidylinositol-4,5-bisphosphate from the inner monolayer might eject some protein from the membrane and thus contract the inner monolayer. Alternatively, these lipids could be involved in some process that influences cell shape independently of the bilayer balance. Inositides are thought to alter the lateral mobility of membrane proteins through their interactions with the cytoskeleton (40). Such interactions might also be related to cell shape, although we agree with the assessment of Lange and co-workers (18) that there is no convincing evidence linking cytoskeletal properties to cell shape.

Relationship to Shape Changes in Ghosts

When human erythrocytes are lysed in Tris buffer and resuspended in isotonic saline containing 1 mM MgATP at 0°C, they first crenate, then slowly recover their discoid shape (10), and eventually become stomatocytic. Several proposals have been made to explain ghost shape changes, some invoking rearrangements of the cytoskeleton (10, 41).

Unless Ca^{2+} is rigorously excluded, erythrocyte lysis is accompanied by breakdown of inositides and phosphatidic acid (26). This observation suggests that Tris lysis produces ghosts that are deficient in inner monolayer phospholipids, which could explain why they crenate at normal ionic strength. The recovery of the normal discoid shape upon incubation with MgATP could arise from resynthesis of the degraded lipids. The work of Fairbanks et al. (13) suggests that synthesis of phosphatidic acid and not phosphatidylino-

sitol-4,5-bisphosphate might be the key event in this recovery.[2] Agents that produce crenation-resistant ghosts (17) might inhibit the degradation of phosphatidic acid or inositides, or might accelerate their resynthesis.

Relationship to Shape Changes in Platelets

The physiological roles of inositide metabolism and crenation in erythrocytes are not yet evident. However, they could be related to apparently similar phenomena that occur during platelet activation (42). Both cells change from smooth disks to spiculate spheres in response to Ca^{2+} loading. Platelets change shape in response to other stimuli as well, including platelet activating factor, a hydrophilic lecithin derivative that would be expected to cause rapid crenation in erythrocytes. In some cases, platelet activation has been correlated with the degradation of phosphatidylinositol-4-phosphate and phosphatidylinositol-4,5-bisphosphate. Both platelets and erythrocytes undergo their shape changes when unfixed cells are placed between a glass microscope slide and coverslip (unpublished observation). Finally, erythrocytes and platelets are derived from a common stem cell, and have similar phospholipid compositions and asymmetries (43). These similarities suggest that a common mechanism might underlie erythrocyte and platelet shape changes. Preliminary experiments in this laboratory suggest that platelet shape is governed by bilayer balance, and that agents that change platelet shape do so by disrupting this balance, either by physical intercalation or by inducing inositide breakdown.

We thank Kong Joo Lee and Katherine Mitchell for assistance with the scanning electron microscopy.

This work was supported by grants from the National Institutes of Health (HL 23787) and the American Heart Association (Grant-in-Aid 80990).

Received for publication 27 October 1983, and in revised form 2 February 1984.

REFERENCES

1. Nakao, M., T. Nakao, and S. Yamazoe. 1960. Adenosine triphosphate and maintenance of shape of human red cells. *Nature (Lond.).* 187:945–946.
2. Sheetz, M. P., and S. J. Singer. 1974. Biological membranes as bilayer couples. A mechanism of drug-erythrocyte interactions. *Proc. Natl. Acad. Sci. USA.* 71:4457–4461.
3. Conrad, M. J., and S. J. Singer. 1981. The solubility of amphipathic molecules in biological membranes and lipid bilayers and its implications for membrane structure. *Biochemistry.* 20:808–818.
4. Chalpin, D. B., and A. M. Kleinfeld. 1983. Interaction of fluorescence quenchers with the n-(9-anthroyloxy) fatty acid membrane probes. *Biochim. Biophys. Acta.* 731:465–474.
5. Matayoshi, E. D. 1980. Distribution of shape-changing compounds across the red cell membrane. *Biochemistry.* 19:3414–3422.
6. Lux, S. E. 1979. Spectrin-actin membrane skeleton of normal and abnormal red blood cells. *Semin. Hematol.* 16:21–51.
7. Lux, S., K. John, and M. Karnovsky. 1976. Irreversible deformation of the spectrin-actin lattice in irreversibly sickled cells. *J. Clin. Invest.* 58:955–963.
8. Yu, J., D. A. Fischman, and T. L. Steck. 1973. Selective solubilization of proteins and phospholipids from red blood cell membranes by nonionic detergents. *J. Supramol. Struct.* 1:233–248.
9. Birchmeier, W., and S. J. Singer. 1977. On the mechanism of ATP-induced shape changes in human erythrocyte membranes. II. The role of ATP. *J. Cell Biol.* 73:647–659.
10. Sheetz, M. P., and S. J. Singer. 1977. On the mechanism of ATP-induced shape changes in human erythrocyte membranes. I. The role of the spectrin complex. *J. Cell Biol.* 73:638–646.
11. Pinder, J. C., D. Bray, and W. B. Gratzer. 1977. Control of interaction of spectrin and actin by phosphorylation. *Nature (Lond.).* 270:752–754.
12. Nelson, M. J., J. E. Ferrell, and W. H. Huestis. 1979. Adrenergic stimulation of membrane protein phosphorylation in human erythrocytes. *Biochim. Biophys. Acta.* 558:136–140.
13. Fairbanks, G., V. P. Patel, and J. E. Dino. 1981. Biochemistry of ATP-dependent membrane shape change. *Scand. J. Clin. Lab. Invest.* 41(Suppl. 156):139–144.
14. Patel, V. P., and G. Fairbanks. 1981. Spectrin phosphorylation and shape change of human erythrocyte ghosts. *J. Cell Biol.* 88:430–440.
15. Anderson, J., and J. M. Tyler. 1980. State of spectrin phosphorylation does not affect erythrocyte shape or spectrin binding to erythrocyte membranes. *J. Biol. Chem.* 255:1259–1265.
16. Brenner, S., and E. Korn. 1979. Spectrin-actin interactions: phosphorylated and dephosphorylated spectrin tetramer crosslink F-actin. *J. Biol. Chem.* 254:8620–8627.
17. Lange, Y., A. Gough, and T. L. Steck. 1982. Role of the bilayer in the shape of the isolated erythrocyte membrane. *J. Membr. Biol.* 69:113–123.
18. Lange, Y., R. A. Hadesman, and T. L. Steck. 1982. Role of the reticulum in the stability and shape of the isolated human erythrocyte membrane. *J. Cell Biol.* 92:714–721.
19. Allan, D., and R. H. Michell. 1975. Accumulation of 1,2-diacylglycerol in the plasma membrane may lead to echinocyte transformation of erythrocytes. *Nature (Lond.).* 258:348–349.
20. Allan, D., and P. Thomas. 1981. Ca^{2+}-induced biochemical changes in human erythrocytes and their relation to microvesiculation. *Biochem. J.* 198:433–440.
21. Lew, V. L. 1971. On the ATP dependence of the Ca^{2+}-induced increase in K^+ permeability of human red cells. *Biochim. Biophys. Acta.* 233:827–830.
22. Bessis, M. 1973. Red cell shapes: An illustrated classification and its rationale. *In* Red Cell Shape. M. Bessis, R. I. Weed, and P. F. LeBlond, editors. Springer-Verlag, New York. 1–23.
23. Ferrell, J. E., and W. H. Huestis. 1982. Calcium does not mediate the shape change that follows ATP depletion in human erythrocytes. *Biochim. Biophys. Acta.* 687:321–328.
24. Kimmich, G. A., J. Randles, and J. S. Brand. 1975. Assay of picomole amounts of ATP, ADP, and AMP using the luciferase enzyme system. *Anal. Biochem.* 69:187–206.
25. Allan, D., R. Watts, and R. H. Michell. 1976. Production of 1,2-diacylglycerol and phosphatidate in human erythrocytes treated with calcium ions and ionophore A23187. *Biochem. J.* 156:225–232.
26. Garrett, N. E., R. J. B. Garrett, R. T. Talwalker, and R. L. Lester. 1976. Rapid breakdown of diphosphoinositide and triphosphoinositide in erythrocyte membranes. *J. Cell. Physiol.* 87:63–70.
27. Bartlett, G. R. 1959. Phosphorus assay in column chromatography. *J. Biol. Chem.* 234:466–468.
28. Allan, D., and R. H. Michell. 1978. A calcium-activated polyphosphoinositide phosphodiesterase in the plasma membrane of human and rabbit erythrocytes. *Biochim. Biophys. Acta.* 508:277–286.
29. Nelson, G. J. 1972. Lipid composition and metabolism of erythrocytes. *In* Blood Lipids and Lipoproteins: Quantitation, Composition, and Metabolism. G. J. Nelson, editor. Wiley Interscience, New York. 317–386.
30. Harris, H. W., N. Levin, and S. E. Lux. 1980. Comparison of the phosphorylation of human erythrocyte spectrin in the intact red cell and in various cell-free systems. *J. Biol. Chem.* 255:11521–11525.
31. Downes, C. P., P. T. Hawkins, and R. H. Michell. 1982. Measurement of the metabolic turnover of the 4- and 5-phosphates of phosphatidylinositol 4,5-bisphosphate in erythrocytes. *Biochem. Soc. Trans.* 10:250–251.
32. Hokin, L. E., and M. R. Hokin. 1963. Diglyceride kinase and other pathways for phosphatidic acid synthesis in the erythrocyte membrane. *Biochim. Biophys. Acta.* 67:470–484.
33. Hokin, L. E., M. R. Hokin, and D. Mathison. 1963. Phosphatidic acid phosphatase in the erythrocyte membrane. *Biochim. Biophys. Acta.* 67:485–497.
34. Downes, C. P., and R. H. Michell. 1982. The control by Ca^{2+} of the polyphosphoinositide phosphodiesterase and the Ca^{2+}-pump ATPase in human erythrocytes. *Biochem. J.* 202:53–58.
35. Wintrobe, M. M. 1981. Clinical Hematology. 8th edition. Lea and Febiger, Philadelphia.
36. Cornell, B. A., and F. Separovic. 1983. Membrane thickness and acyl chain length. *Biochim. Biophys. Acta.* 733:189–193.
37. Allan, D., P. Thomas, and R. H. Michell. 1978. Rapid transbilayer diffusion of 1,2-diacylglycerol and its relevance to control of membrane curvature. *Nature (Lond.).* 276:289–290.
38. Beck, J. S. 1978. Relations between membrane monolayers in some red cell shape transformations. *J. Theor. Biol.* 75:487–501.
39. Lange, Y., and J. Slayton. 1982. Interaction of cholesterol and lysophosphatidylcholine in determining red cell shape. *J. Lipid Res.* 23:1121–1127.
40. Sheetz, M. P., P. Febbroriello, and D. E. Koppel. Triphosphoinositide increases glycoprotein lateral mobility in erythrocyte membranes. *Nature (Lond.).* 296:91–93.
41. Johnson, R. M., G. Taylor, and D. B. Meyer. 1980. Shape and volume changes in erythrocyte ghosts and spectrin-actin network. *J. Cell Biol.* 86:371–376.
42. Rittenhouse, S. E. 1982. Inositol lipid metabolism in the responses of stimulated platelets. *Cell Calcium.* 3:311–322.
43. Chap, H. J., R. F. A. Zwaal, and L. L. M. van Deenen. 1977. Action of highly purified phospholipases on blood platelets: evidence for an asymmetrical distribution of phospholipids in the surface membrane. *Biochim. Biophys. Acta.* 467:146–164.

[2] It should be emphasized that although reference 13 argues against a role for inositide phosphorylation in the echinocyte to discocyte shape change of ghosts, it does not conflict with the present work on intact cells.